JOURNAL OF SOLID STATE CHEMISTRY 50, 263–272 (1983)

Study of Protonic Diffusion in Hydrogen Uranyl Phosphate Using a Pulsed Field Gradient NMR Method*

Y.-T. TSAI,† W. P. HALPERIN, AND D. H. WHITMORE‡

Departments of Materials Science and Engineering and Physics, Northwestern University, Evanston, Illinois 60201

Received March 7, 1983; in revised form July 18, 1983

The diffusion of ^1H in the fast protonic conductor $H(UO_2PO_4) \cdot 4H_2O$ has been investigated as a function of temperature by employing pulsed field gradient NMR measurements. In the light of the present diffusion results and published conductivity observations on the same compound, it is likely that protonic diffusion and conductivity in this material occur by the same mechanism. Possible mechanistic processes for the proton motion in this material which are consistent with the activation energy for protonic diffusion found in this study are briefly discussed.

I. Introduction

The compound hydrogen uranyl phosphate, $H(UO_2PO_4) \cdot 4H_2O$ (hereafter designated as HUP), is one of the few compounds which exhibits unusually high proton conductivity ($\sigma = 4 \times 10^{-3}\ (\Omega\ \text{cm})^{-1}$ at 290 K) (*1*) and yet can be easily fabricated into dense disks or films suitable for use in electrochromic displays, fuel cells, or hydrogen gas sensors (*2–4*).

Structural investigations of HUP (*5*) have shown that a phase transition from tetragonal (type I) to orthorhombic (type II) symmetry occurs below 274 K, the HUP(I) phase existing above 274 K being the exceptionally good proton conductor. The unit cell of HUP(I) contains two $(UO_2PO_4)_n^{n-}$ framework layers separated by interlayers containing water and a linked H-bond network (*1, 5*). Howe and co-workers have carried out a series of detailed studies on the ionic conductivity (*1, 6, 7*), the thermal stability (*8*), and NMR relaxations (*9*) of HUP with a view towards understanding the protonic transport mechanism in the material.

The picture that emerged from the foregoing studies delineated the following features for HUP: (1) the presence of mobile protons; (2) the presence of a two-dimensional, continuous network of water molecules; (3) rapid rotation of water molecules; and (4) the absence of basic (negatively charged) sites which could act as proton traps. Shilton and Howe (*1*) suggested that the protonic conduction mechanism for

* Work supported by the U.S. Dept. of Energy under contract DE-AC02-76ERO2564. This work is based in part on a thesis submitted by Y.-T. Tsai for the Ph.D. degree at Northwestern University, June, 1983.

† Now with Technics West Inc., San Jose, Calif. 95131.

‡ Author to whom correspondence should be addressed.

0022-4596/83 $3.00

HUP might be similar to the well-known Grotthus mechanism found in aqueous acid solutions, namely, a cooperative intermolecular proton transfer between adjacent water molecules, followed by a rate-determining rotation step for the water molecule. This was based on the observation of a higher activation energy for protonic conduction than that found for the spin–lattice (T_1) and spin–spin (T_2) NMR relaxations. It is reasonable to expect that dehydration of HUP might destroy the conduction network for the protons, thereby causing a diminution in ionic conduction. In fact, it has been observed that HUP dehydrates at a temperature slightly above 353 K to yield a poorly conducting phase.

Recently, Bernard *et al.* (*10*) inferred, from neutron diffraction evidence, diffusion and conduction mechanisms in the compound $DUO_2AsO_4 \cdot 4D_2O$ (DUAs), a fast proton conductor which is structurally similar to HUP. Their neutron diffraction investigation revealed that partial ordering occurred in the DUAs structure, along with $D_5O_2^+$ ions, D_4O_2 dimers, and vacancies. They suggested that the activation energy for diffusion should involve the energy for a $D_5O_2^+$ ion rotation as well as that for the $D_5O_2^+$-vacancy hopping process; in contrast, the activation energy for conduction should depend on both the energy for $D_5O_2^+$-vacancy hopping process and the energy for the D_4O_2 dimer-vacancy rotation. Since the energy for the $D_5O_2^+$ ion rotation will almost certainly be lower than that for the D_4O_2 dimer rotation, Bernard *et al.* (*10*) argued that a lower activation energy should be found for diffusion than for conduction.

To reinforce this contention, they noted that the activation energy for conductivity in HUP was found to be 0.31 ± 0.01 eV (*7*), whereas an activation energy value for diffusion in HUP, inferred from NMR measurements of T_1 and T_2 (*9*) and pulsed field gradient NMR diffusivity data (*11*) (three experimental points), was found to be 0.21 ± 0.01 eV. In the light of the uncertainties generally found in activation energy values for diffusion derived from T_1 and T_2 NMR relaxation data and the sparsity and preliminary nature of the published proton diffusion data existing for HUP, its inaccuracy and the extremely limited range of temperature over which these diffusion measurements were made, it remains an open question whether there are indeed separate mechanisms operating for conduction and diffusion in the particle-hydrate group (*12*) of fast proton conductors exemplified by HUP, HUAs, and DUAs.

Here, we report on an improved NMR pulsed field gradient method for the measurement of diffusion coefficients greater than about 10^{-8} cm^2 sec^{-1} in condensed phases and its application to the systematic observation of proton diffusivities in the layered compound HUP. In addition, we discuss the general implications of our diffusion findings in HUP with respect to possible mechanisms of proton transport in those particle-hydrate materials which exhibit fast proton conduction.

II. Experimental Procedure

(*1*) *Sample Preparation*

Hydrogen uranyl phosphate (HUP) slurries, obtained from A. T. Howe, were prepared by a method previously described (*6*) and were derived from the same batch used in the investigation by Childs *et al.* (*9*). Powder samples of HUP were prepared by drying the slurry on a filter paper, followed by saturating the dried powder with water vapor at 1 atm pressure and a temperature of 298 K over a 14-day period. The resulting (saturated) samples of HUP were sealed in 4-mm-i.d., spectroscopic grade, NMR tubes to prevent the loss of water.

(*2*) *The NMR Spectrometer*

The NMR spectrometer used in this investigation was a modified version of the

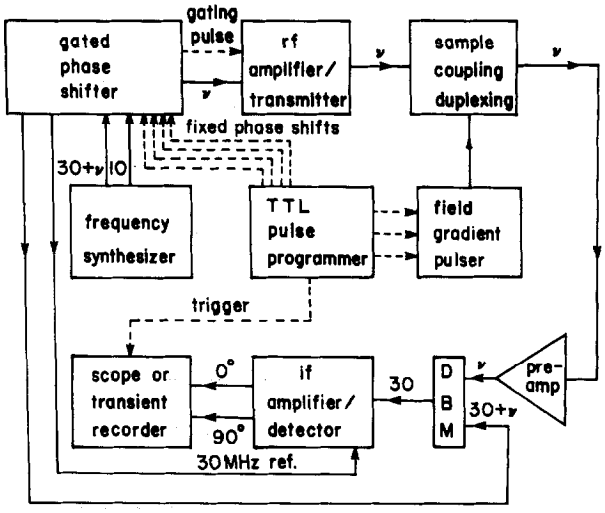

FIG. 1. Schematic diagram of the pulsed NMR spectrometer.

spectrometer design reported by Gibson *et al.* (*13*) and was operated at a frequency of 25.3 MHz throughout the present measurements. A schematic diagram of the spectrometer is shown in Fig. 1, the frequencies shown therein being in megahertz. The Programmed Test Sources Model PTS 160 frequency synthesizer is a radio frequency (rf) source which generates a continuous sinusoidal wave of frequency $(30 + \nu)$ MHz where ν is the Larmor frequency for the nuclei of interest at a given magnetic field. The gating and phase shifting of the rf pulse were accomplished by the gated phase shifter (GPS) at an intermediate frequency, 30 MHz, which has been derived from the 10-MHz reference output of the frequency synthesizer. The lower sideband output of a single sideband mixer in the GPS delivered an rf pulse with a frequency of 25.3 MHz.

The duration of the rf pulse was controlled by an Interface Technology RS-648E pulse programmer. Typically, the rf output of the GPS is about 0.5 V and must be amplified to some desired level, usually several thousand volts by an Arenberg PG-650C amplifier/transmitter. The amplified rf pulse was coupled to an rf coil surrounding the sample where the NMR signal, typically of the order of several microvolts, was fed into a Matec 253 preamplifier. The amplified NMR signal was then mixed with a $(30 + \nu)$ MHz reference signal, thereby resulting in 30 MHz and $(30 + 2\nu)$ MHz components; only one of these component signals (30 MHz) was amplified by the 30-MHz narrow-band amplifier of the receiver.

Quadrature outputs of the NMR signal (0 and 90°) were separated by a phase comparator and then amplified with the aid of dc amplifiers and filters. These outputs were digitized by a Nicolet Explorer 2090-III transient recorder and the digitized signals were then fed into a Z-80 microcomputer where the signals were averaged and the echo amplitude was computed as the square root of the sum of two squared quadrature outputs. A nonlinear, least-squares fitting computer program was employed to determine the echo amplitude and its associated standard error.

A field-gradient pulser was used to generate the time-dependent, magnetic-field gradients which are essential for the pulsed-field gradient (PFG) diffusion experiments. The duration of the gradient pulses was programmed by the TTL pulse programmer and the magnitude of the field gradient was

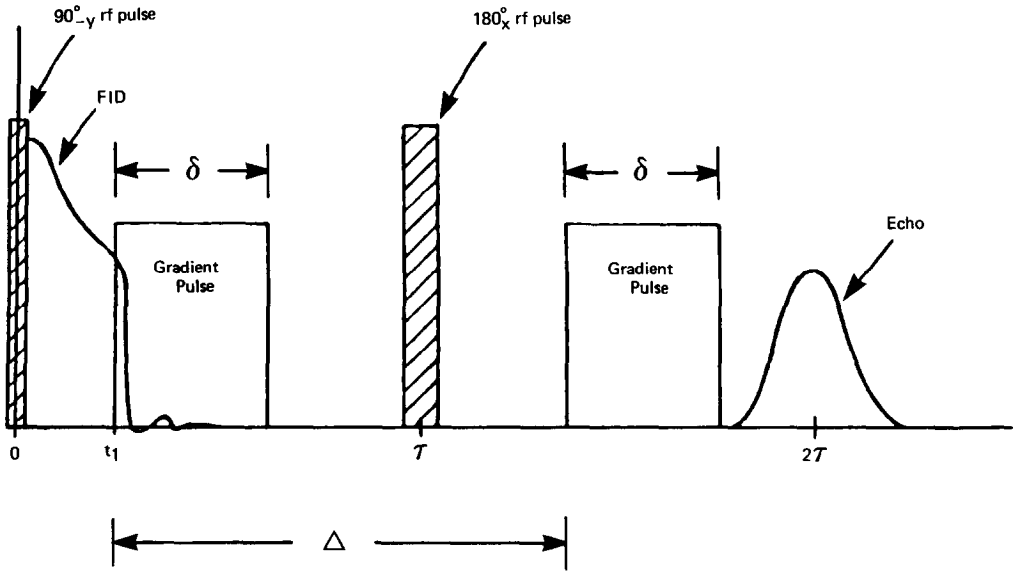

FIG. 2. The Stejskal–Tanner pulsed-field gradient, spin-echo sequence.

monitored through measurement of the strength of the current pulse. The current pulser and quadrupole coil employed were similar to those described by Karlicek and Lowe (*14*).

3. Pulsed-Field Gradient NMR Measurements

The Stejskal–Tanner (*15*) pulsed-field gradient, spin-echo sequence, shown in Fig. 2, was employed in the present proton diffusion measurements. Under isothermal conditions, a 90° rf pulse was applied to the sample at time $t = 0$ which was followed by a field gradient pulse, of duration δ, at $t = t_1$. At time $t = \tau$, a 180° rf pulse was applied which was followed at time $t = (t_1 + \Delta)$ by a second field gradient pulse that was carefully adjusted to be identical to the first. A spin-echo signal occurred at a time $t = 2\tau$ and the attenuation of the spin echo, undergoing unrestricted diffusion on the time scale of Δ, is given by (*15*)

$$\ln [A(2\tau)^*/A(2\tau)] = -\gamma^2 D G^2 \delta^2 (\Delta - \delta/3). \quad (1)$$

Here $A(2\tau)^*$ and $A(2\tau)$ are, respectively, the spin-echo amplitudes in the presence and in the absence of the gradient pulses of magnitude G, γ the gyromagnetic ratio of the proton, δ the duration of a gradient pulse, Δ the time interval between the start of the two gradient pulses, and D the protonic diffusion coefficient for the sample.

Proton diffusion in HUP is generally believed to occur within a two-dimensional network of water molecules. Furthermore, the samples investigated here were polycrystalline. Accordingly, on the average, diffusion should be restricted in the sense that the diffusion path in the direction of the gradient magnetic field is constrained. A complete theoretical account of this regime for arbitrary times δ and Δ has not yet appeared in the literature; however, it can be shown that the echo-amplitude ratio $A^*(2\tau)/A$ is given by

$$\langle \exp - \gamma^2 D G^2 \cos^2\theta \delta^2 (\Delta - \delta/3) \rangle_\theta$$

where $\langle\ \rangle_\theta$ indicates a powder average over all solid angles. The above average has the

same form as the well-known error function. Calculation of the diffusion coefficient D requires the solution of an integral equation which can be accomplished numerically. In the limit of small D and short times (δ), it is sufficient to replace G^2 in Eq. (1) by $G^2/3$. In this case, the diffusion coefficient can be determined from the slope of a plot of $\ln [A(2\tau)^*/A(2\tau)]$ vs $\delta^2(\Delta - \delta/3)$ because γ and G are known quantities, the latter having been measured by means of the independent calibration experiments described below.

The magnitude of the magnetic field gradient was calibrated using the following methods: (a) lineshape analysis of free-induction decay (FID) signals in the presence of a constant gradient (*16*), and (b) measurements of the protonic diffusion coefficient by our PFG method in substances, such as water, glycerol, and *N*-decanol, for which published diffusivity values are available spanning the range for $D_{^1H}$ in HUP determined in our experiments.

The field gradient measurement by lineshape analysis was accomplished by inserting a cylindrical sample in a constant gradient and observing the FID shape of a spin echo for a 90–180°-echo sequence. If it is assumed that G is constant over the entire sample, the time dependence of the magnetization M is given by (*16*)

$$M(t) = M_0[2J_1(\gamma GRt)/(\gamma GRt)] \qquad (2)$$

where R is the radius of the cylindrical sample, t the time with zero defined to be at the echo peak, and $J_1(\gamma GRt)$ the first-order Bessel function. By determining the zero values of $J_1(\alpha)$ and the corresponding values of time t, one can obtain a value of G by equating

$$\alpha_i = \gamma GRt_i \qquad (3)$$

since γ, t_i, α_i, and R are known quantities.

The field gradient calibration, based on measuring protonic diffusion coefficients in water, glycerol, and *N*-decanol, proceeded by first observing the amplitude ratio $A(2\tau)^*/A(2\tau)$ and then substituting into Eq. (1) the published value of D at the measuring temperature for the given substance and solving Eq. (1) for G. These measurements were carried out on the three aforementioned substances at 25.3 MHz, a Δ value of 10.01 msec and a gradient current of 4.3 A being used.

The pulsed field gradient protonic diffusion measurements on HUP were performed over a temperature range of 298.5 to 345 K using a frequency of 25.3 MHz, a field gradient of 215 G cm^{-1}, and a gradient separation (Δ) of 6.01 msec. The temperature of the HUP sample was stabilized to within ± 0.5 of the measuring temperature with the aid of a temperature controller and a thermocouple.

It was found that significant heating results when large pulsed currents are applied to the quadrupole coil. In our present design, this heat is shunted from the neighborhood of the sample to a temperature-regulated, large copper block. This was achieved by winding the quadrupole coil in a copper coil former which was directly attached to the aforementioned thermal reservoir. The former was designed such that there were minimal effects on the magnetic field pulses from induced screening currents. In addition, the temperature of the sample was monitored by an independent thermocouple mounted very close to the sample.

Several common problems associated with echo stability were resolved with the technique applied in this work. Instability in the echo is frequently observed in pulsed magnetic field gradient measurements resulting from coupling between the pulsed field and the iron core of the steady magnet or between the pulsed field and the field regulation sensors for the homogeneous applied field. This can be alleviated by computing the square root of the sum of the squares of the two quadrature outputs of

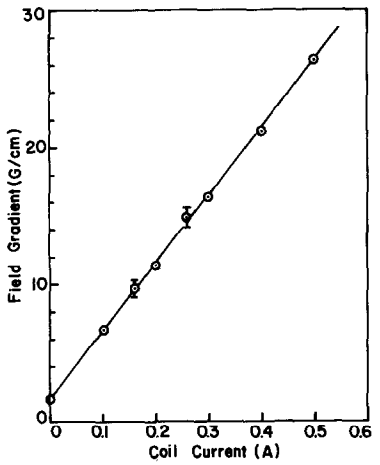

FIG. 3. Gradient calibration by lineshape analysis of FID.

the receiver and signal averaging channel by channel. Furthermore, the root-mean sum of the squares of these quadrature outputs produces an echo envelope whose shape remains independent of drift or fluctuations in the applied homogeneous magnetic field. A disadvantage of this approach is that significant time (≈5 sec) is required for the computation of each point. Using more sophisticated computational techniques and a faster microcomputer should reduce this computational time by more than an order of magnitude.

III. Results and Discussion

The results of the lineshape analysis of the FID signals to obtain the field gradient G are depicted in Fig. 3. Up to a coil current of 500 mA, the field gradient was proportional to the current with a slope of 48.9 G/cm-A, the residual-field gradient of the magnet being 1.75 G/cm. In addition, the pulsed-field gradient was calibrated by means of measurements on Cu_2SO_4-doped H_2O at 298 K and on glycerol at 303 K. The results are shown in Figs. 4 and 5. Using published values for the protonic diffusion coefficients in H_2O (2.23×10^{-5} cm^2 sec^{-1} at 298 K) and in glycerol (3.20×10^{-8} cm^2 sec^{-1} at 303 K), the magnitudes of the field gradients were determined to be 206 and 213 G cm^{-1}, respectively, at a gradient current of 4.3 A. These values compare favor-

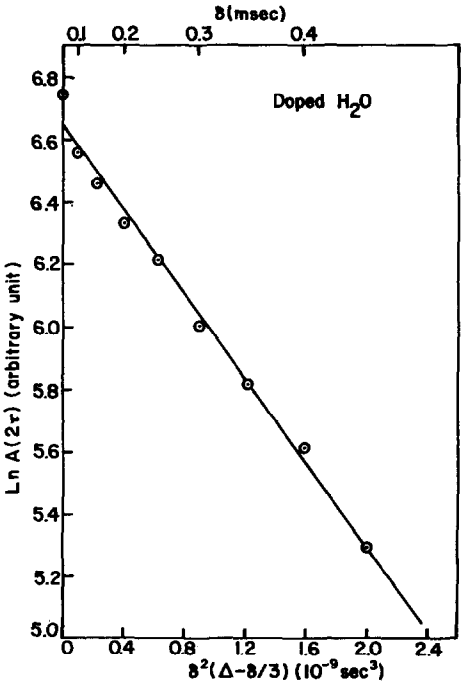

FIG. 4. Plot of diffusion data for doped H_2O at 25°C.

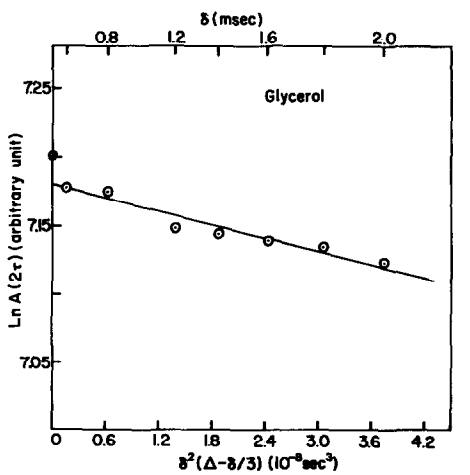

FIG. 5. Plot of diffusion data for glycerol at 30°C.

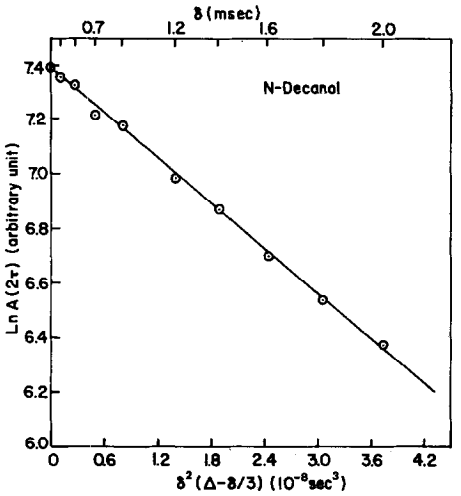

FIG. 6. Plot of diffusion data for *N*-decanol at 30°C.

ably with the value (212 G cm^{-1}) extrapolated from lineshape analysis. A protonic diffusion coefficient for *N*-decanol was determined to be 8.30×10^{-7} cm^2 sec^{-1} at 303 K (see Fig. 6), a value which is in good agreement with the published value of 7.5×10^{-7} cm^2 sec^{-1} for a slightly lower temperature (298 K).

The initial sharp decrease in the amplitude of the echo signal for very small δ as seen, for example, in Figs. 4 and 5 appears to be an experimental artifact which is not clearly understood at this time.

Nine values of the protonic diffusion coefficient in HUP were measured in the range 298.5 to 345 K, using a field gradient of 215 G/cm and a separation of 6.01 msec between the gradient pulses. Typical plots of ln $A(2\tau)$ vs $\delta^2(\Delta - \delta/3)$ at fixed diffusion temperature are shown in Figs. 7 and 8. When the echo-amplitude ratio, $A^*(2\tau)/A(2\tau)$, is smaller than 0.90, a plot of the echo amplitude versus $\delta^2(\Delta - \delta/3)$ will be significantly nonlinear for the case of restricted diffusion, as shown by the dashed and dot-dashed lines in Fig. 8. All of the present PFG measurements show a distinctly linear relation even when the echo-amplitude ratio is as small as 0.67. Our interpretation of this is that protonic diffusion in HUP is unrestricted. Consequently, we have used Eq. (1) to analyze our data which is summarized in the Arrhenius plot of Fig. 9.

The temperature dependence of the proton diffusion coefficients observed here is displayed in this figure. Figure 9 also shows, for comparison, the three protonic diffusion coefficients for HUP measured earlier by Gordon *et al.* (*11*). These *D* values, however, are shown as they would appear if analyzed using Eq. (1) rather than as originally reported. It is evident that the activation energy deduced from our work is consistent with the earlier, less accurate measurements of Gordon *et al.* (*11*); nevertheless, it is noteworthy that our measured diffusion coefficients are approximately three times larger than those given by Gordon *et al.* It should be noted that great care was exercised here in carrying out the calibration procedures for determining the magnitude of the gradient field which yielded the four independent and self-consistent results presented earlier. A least-

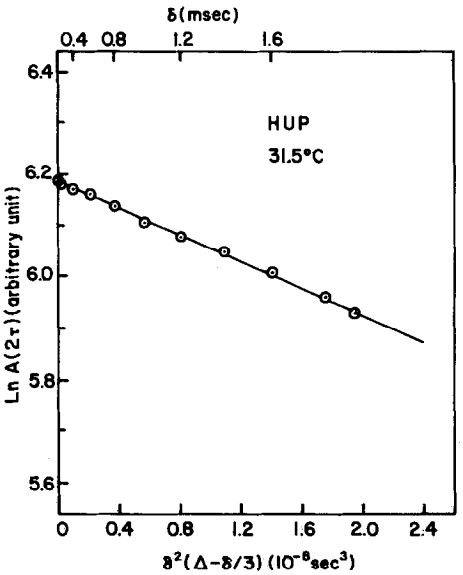

FIG. 7. Plot of diffusion data for HUP at 31.5°C.

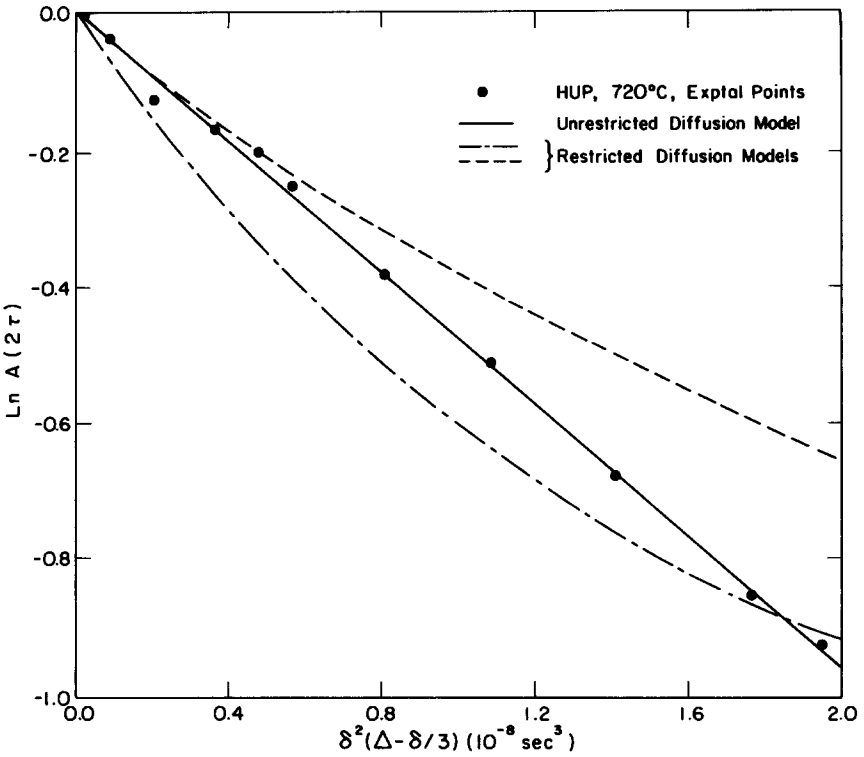

FIG. 8. Plot of diffusion data for HUP at 72°C. The dashed line is the result of a calculation for the case of restricted diffusion where $D = 4.2 \times 10^{-6}$ cm²/sec. The dot-dashed line corresponds to the case of restricted diffusion where $D = 7.6 \times 10^{-6}$ cm²/sec. The solid line gives the expected result for unrestricted diffusion where $D = 1.4 \times 10^{-6}$ cm²/sec.

squares analysis of the present results yielded the following Arrhenius expression for D_{1_H} in HUP:

$$D_{1_H} = (1.177 \pm 0.030) \times 10^{-2} \exp\left[-\frac{(0.269 \pm 0.021 \text{ eV}}{kT}\right] \quad (4)$$

where k is the Boltzmann constant and D_{1_H} is expressed in units of cm² sec^{-1}.

The NMR relaxation time measurements of Childs *et al.* (*9*) suggest an activation energy of 0.21 eV for proton motion in HUP in contrast with our finding of 0.27 eV from the pulsed-field gradient measurements. There are a number of possibilities which might account for this discrepancy. Most importantly, a full understanding of the relationship between the microscopic dynamical behavior expressed by relaxation times and the macroscopic effects of diffusion can be achieved *only* after relaxation experiments are conducted over a wide range of temperature and frequency (i.e., $\omega\tau \ll 1$ and $\omega\tau \gg 1$, where ω is the NMR frequency and τ the correlation time). Since the T_1, T_2 relaxation measurements by Childs *et al.* (*9*) on HUP were carried out over a narrow range of temperature at a single NMR frequency, it is our contention that there are simply insufficient NMR relaxation data available from the study of Childs *et al.* on HUP to establish any meaningful connection between the proton diffusion results of our PFG study and the temperature dependence of this earlier T_1, T_2 relaxation data.

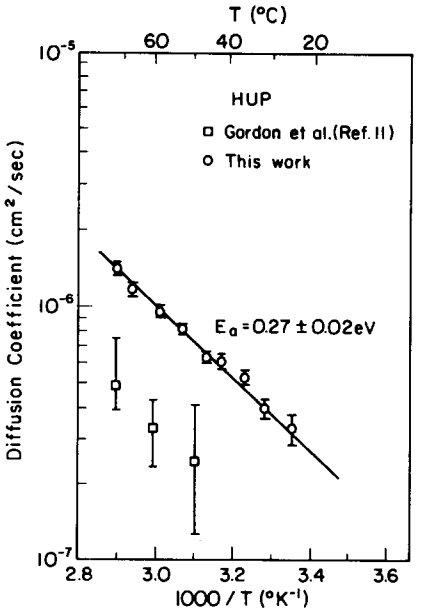

FIG. 9. Arrhenius plot of the protonic diffusion coefficients for HUP.

Because of the magnitude of the activation energy (0.27 eV) given in Eq. (4) for proton diffusivity in HUP and the fact that it is nearly the same (at least when consideration is taken of the experimental uncertainties involved) as that found for HUP by Howe and associates (*1, 6, 7*) in their studies of protonic conductivity (0.31 eV), considerable doubt is now shed on the proposal by Bernard *et al.* (*10*) that separate mechanisms for protonic conduction and diffusion should operate in a particle-hydrate phase like HUP. If, indeed, the proposal by Bernard *et al.* were valid for HUP, one should expect different activation energies for the two transport processes and, moreover, that the activation energy for proton diffusion in HUP would be substantially lower than that for conduction.

Beyond this, we can only state that the activation energy observed here is not inconsistent with that which might be expected from a Grotthus mechanism in which the protons move in two steps: (a) the translation of a proton from an oxonium ion to a water molecule by tunneling in a hydrogen bond, and (b) subsequent reorientation (rotation) of the water molecule thus formed in order to be able to take up the next proton. Since the rotation step (b) is thought to be the slower step in this mechanism, it should be rate determining and the activation found for this mechanism should, therefore, correspond to that for the necessary hydrogen-bond breaking involved in such a step.

While the activation energy (0.27 eV) given in Fig. 9 is a reasonable value for such a bond-breaking rotational process, it should be noted that this value may likewise be a reasonable one for the vehicular mechanism of proton motion in solids suggested by Kreuer *et al.* (*19*). In this vehicular model, the proton does not migrate as H^+ but as OH_3^+, bonded to the water molecule "vehicle," the "unladen" vehicles moving in the opposite direction. The vehicle shows a diffusion coefficient corresponding to that which would be predicted from proton conduction and behaves like a proton acceptor with respect to its crystallographic environment. The results of the present investigation do not allow one to discern which of these two mechanisms (Grotthus or vehicle) is the more likely for proton migration in HUP; further experimentation will be required to elucidate this question of mechanism. For example, if the vehicular mechanism were important in the protonic migration process in HUP, a measurement of ^{18}O self-diffusivity in this material should reveal this since the migration of the water molecule to which an OH_3^+ ion is bonded would be rate controlling.

Crystallographic evidence (*20*) indicates that the waters of hydration in HUP are confined to a two-dimensional structure. Our finding that protonic diffusion in HUP is unrestricted suggests that during the time scale of our measurements, ~12 msec, diffusion is essentially three-dimensional.

This apparent inconsistency possibly may be accounted for if the grain size of our HUP sample is much smaller than the diffusion length during an experiment, ~2 μm. In such a case, proton diffusion would also involve motion of the diffusing species along the grain or particle boundaries which might be the rate-limiting step. Measurements on single crystals of HUP will be necessary to unambiguously establish this possibility.

Finally, it seems worthwhile to stress here that the present investigation has satisfactorily demonstrated the real potential of the pulsed-field gradient NMR technique for the nondestructive, direct, and accurate determination of diffusion coefficients in solid ceramic phases. Indeed, the present work has shown that, using the NMR equipment described here under favorable circumstances, one may observe a proton diffusion coefficient in HUP greater than 10^{-8} cm^2 sec^{-1}. The important material parameter which determines the smallest observable mobile species diffusion coefficient with such a technique is the spin–spin relaxation time (T_2), since this determines the largest available pulse separation. Improvements in the design and construction of the probe, the current pulser, and the rf shielding used in this study, for example, should help minimize systematic errors in the diffusion measurements which arise from an imbalance of the gradient pulses, variations in the field and/or frequency, and instabilities in the amplitude and position of the spin echo.

Acknowledgments

The authors thank A. T. Howe for kindly supplying them with the HUP sample used in this investigation. The considerable help of J. R. Owers-Bradley in the design and construction of the NMR pulsed-field gradient apparatus used here and in the early phases of this study is gratefully acknowledged. We also thank Dr. J. C. Tarczon for helpful discussions regarding restricted diffusion. This work was carried out in the NMR central facility of the Materials Research Center at Northwestern University.

References

1. A. T. Howe and M. G. Shilton, *J. Solid State Chem.* **28,** 345 (1979).
2. P. E. Childs, A. T. Howe, and M. G. Shilton, *J. Solid State Chem.* **34,** 341 (1980).
3. A. T. Howe, S. H. Sheffield, P. E. Childs, and M. G. Shilton, *Thin Solid Films* **67,** 365 (1980).
4. J. S. Lundsgaard, J. Malling, and M. L. S. Birchall, *Solid State Ionics* **7,** 53 (1982).
5. M. G. Shilton and A. T. Howe, *J. Solid State Chem.* **34,** 137 (1980).
6. M. G. Shilton and A. T. Howe, *Mater. Res. Bull.* **12,** 701 (1977).
7. A. T. Howe and M. G. Shilton, *J. Solid State Chem.* **34,** 149 (1980).
8. A. T. Howe and M. G. Shilton, *J. Solid State Chem.* **31,** 393 (1980).
9. P. E. Childs, T. K. Halstead, A. T. Howe, and M. G. Shilton, *Mater. Res. Bull.* **13,** 609 (1978).
10. L. Bernard, A. Fitch, A. F. Wright, B. E. Fender, and A. T. Howe, *Solid State Ionics* **5,** 459 (1981).
11. R. E. Gordon, J. H. Strange, and T. K. Halstead, *Solid State Commun.* **31,** 995 (1979).
12. W. A. England, M. G. Cross, A. Hammett, P. J. Wiseman, and J. B. Goodenough, *Solid State Ionics* **1,** 231 (1980).
13. A. V. Gibson, J. R. Owers-Bradley, I. D. Calder, J. B. Ketterson, and W. P. Halperin, *Rev. Sci. Instrum.* **52,** 1509 (1981).
14. R. F. Karlicek, Jr., and I. J. Lowe, *J. Magn. Reson.* **37,** 75 (1980).
15. E. O. Stejskal and J. E. Tanner, *J. Chem. Phys.* **42,** 288 (1965).
16. J. S. Murdy, *J. Magn. Reson.* **10,** 11 (1973).
17. C. H. Everhart and C. S. Johnson, Jr., *J. Magn. Reson.* **48,** 466 (1982).
18. K. D. Kreuer, A. Rabenau, and W. Weppner, *Angew. Chem. Int. Ed. Engl.* **21,** 208 (1982).
19. K. D. Kreuer, W. Weppner, and A. Rabenau, *Solid State Ionics* **3/4,** 353 (1981).
20. B. Morosin, *Phys. Lett. A* **65,** 53 (1978).